Evaluation of lipid-binding properties of the N-terminal helical segments in human apolipoprotein A-I using fragment peptides

Masafumi Tanaka,[a]* Toshitaka Tanaka,[a] Shinya Ohta,[a] Toru Kawakami,[b] Hiroyuki Konno,[c] Kenichi Akaji,[c] Saburo Aimoto[b] and Hiroyuki Saito[a]

Although the N-terminal region in human apolipoprotein (apo) A-I is thought to stabilize the lipid-free structure of the protein, its role in lipid binding is unknown. Using synthetic fragment peptides, we examined the lipid-binding properties of the first 43 residues (1–43) of apoA-I in comparison with residues 44–65 and 220–241, which have strong lipid affinity in the molecule. Circular dichroism measurements demonstrated that peptides corresponding to each segment have potential propensity to form α-helical structure in trifluoroethanol. Spectroscopic and thermodynamic measurements revealed that apoA-I (1–43) peptide has the strong ability to bind to lipid vesicles and to form α-helical structure comparable to apoA-I (220–241) peptide. Substitution of Tyr-18 located at the center of the most hydrophobic region in residues 1–43 with a helix-breaking proline resulted in the impaired lipid binding, indicating that the α-helical structure in this region is required to trigger the lipid binding. In contrast, apoA-I (44–65) peptide exhibited a lower propensity to form α-helical structure upon binding to lipid, and apoA-I (44–65/S55P) peptide exhibited diminished, but not completely impaired, lipid binding, suggesting that the central region of residues 44–65 is not pivotally involved in the formation of the α-helical structure and lipid binding. These results indicate that the most N-terminal region of apoA-I molecule, residues 1–43, contributes to the lipid interaction of apoA-I through the hydrophobic helical residues. Copyright © 2008 European Peptide Society and John Wiley & Sons, Ltd.

Keywords: apoA-I; peptide-lipid interaction; synthetic peptide; proline substitution

Introduction

High-density lipoprotein (HDL) and apolipoprotein (apo) A-I, the major protein constituent of HDL, are inversely related to risk of cardiovascular disease in humans through their role in the reverse cholesterol transport pathway [1]. In this pathway, lipid-free or lipid-poor apoA-I molecules remove cholesterol from peripheral cells and transport it in the form of HDL back to the liver for excretion [2]. Therefore, apoA-I and its mimetic peptides are thought to be potential therapeutic agents for cardiovascular disease [3]. In fact, human clinical trials are now being carried out using apoA-I mimetic peptide [4].

Computational analysis of the amino acid sequence of human apoA-I (243 amino acids) reveals that residues 44–243, encoded by exon 4, contain eight 22-mer and two 11-mer amphipathic α-helices mostly punctuated by proline (P) residues [5]. These α-helices are classified as either class A or Y based on the distribution of positively and negatively charged amino acids. Studies of synthetic peptides corresponding to these amphipathic α-helices have shown that the helices spanning either residues 44–65 or 220–241 have the greatest lipid affinity [6,7]. In addition, peptide containing either of these two segments can mediate ATP-binding cassette transporter A1-dependent cholesterol removal [8]. In contrast, residues 1–43, encoded by exon 3, contain the only class G* helix present in the protein [5]. The amino acid sequence of this segment is highly conserved among species and therefore, thought to play some distinctive roles [9,10]. However, the structural and functional significances of this segment have not been fully elucidated.

Lipid-free apoA-I is folded into two domains, comprising an N-terminal part (residues around 1–189) forming a four-helix bundle and a less organized C-terminal part (residues around 190–243) [11–13]. ApoA-I is thought to initially bind to lipid through the C-terminal domain, followed by a conformational opening of the helix bundle in the N-terminal domain. According to hydropathy plot analysis of apoA-I, the segments spanning residues either 1–43 or 220–241 are highly hydrophobic centered around tyrosine (Y) 18 or leucine (L) 230, respectively [10]. Substitution of L230 with P residue, which is known to disrupt the helical structure of a protein [14], diminished the lipid binding. In contrast, substitution of Y18 with P residue decreased the stability of the N-terminal

*   Correspondence to: Masafumi Tanaka, Department of Biophysical Chemistry, Kobe Pharmaceutical University, 4-19-1 Motoyamakita-machi, Higashinada-ku, Kobe 658-8558, Japan. E-mail: masatnk@kobepharma-u.ac.jp

a   Department of Biophysical Chemistry, Kobe Pharmaceutical University, Kobe 658-8558, Japan

b   Laboratory of Protein Organic Chemistry, Institute for Protein Research, Osaka University, Suita 565-0871, Japan

c   Department of Chemistry, Graduate School of Medical Science, Kyoto Prefectural University of Medicine, Kyoto 603-8334, Japan

bundle structure [15], suggesting that the most N-terminal region of apoA-I is important for maintaining the bundle structure [15]. In the present study, synthetic peptides corresponding to apoA-I sequence were studied to elucidate the roles of the putative N-terminal helical segments in lipid binding.

Materials and Methods

Materials

Fmoc amino acid derivatives were obtained from Peptide Institute, Inc. (Minou, Japan), and were used without further purification. Egg phosphatidylcholine (PC) was purchased from Sigma-Aldrich (St. Louis, MO). Dimyristoylphosphatidylcholine (DMPC) was from NOF (Tokyo, Japan). All other reagents were special grade.

Peptide Synthesis

Primary sequences of the synthetic peptides used in the present study are listed in Table 1. Peptides were synthesized on a 0.25 mmol scale using Fmoc chemistry. The N- and the C-termini were capped with an acetyl group and an amide group, respectively. Peptides were cleaved from the resin using standard trifluoroacetic acid methods and purified by high-performance liquid chromatography. Matrix-assisted laser desorption ionization mass spectrometry was measured using either a Bruker Autoflex or an Applied Biosystems Voyager-DE PRO to check the molecular weights of synthetic peptides. In all experiments, peptides were freshly dialyzed from 6 M guanidine hydrochloride solution into the appropriate buffer before use. Peptide concentrations were determined by the Lowry procedure using bovine serum albumin (Bio-Rad) as a standard.

Preparation of Lipid Vesicles

A film of egg PC or DMPC on the wall of a glass tube was dried under vacuum overnight and hydrated with buffer. Egg PC small unilamellar vesicles (SUV) with a diameter of approximately 25 nm, were prepared by sonication and then ultracentrifuged in a Beckman TLA110 rotor (51 000 rpm) for 2 h to remove larger particles and titanium debris as described [16]. Bilayer vesicles of DMPC were prepared by the extrusion method using a Liposo-Fast extrusion apparatus (Avestin Inc., Canada) through 200-nm filters as described [17]. The PC concentration was determined using an enzymatic assay kit for choline from Wako (Osaka, Japan).

Circular Dichroism Spectroscopy

Circular dichroism (CD) spectra of apoA-I peptides were obtained using an Aviv 62ADS spectropolarimeter at 50 μg/ml. Peptide samples were dissolved either in 10 mM sodium phosphate buffer (pH 7.4) or in 80% 2,2,2-trifluoroethanol (TFE). CD spectra in the presence of egg PC SUV were also measured. Molar ellipticity ($[\theta]$) was calculated from the equation: $[\theta] = (MRW) \, \theta/10lc$, where θ is a measured ellipticity in degrees, l is the cuvette path length (0.2 cm), and c is the peptide concentration in g/ml, and the mean residue weight (MRW) obtained from the molecular weight and the number of amino acids. The α-helix contents were calculated from the equation using $[\theta]$ at 222 nm: % α-helix = $[(-[\theta]_{222} + 3000)/(36\,000 + 3000)] \times 100$ [15]. For lipid-binding experiments, apoA-I peptide was incubated with SUV (lipid/peptide = 100/1 (w/w)) for 1 h prior to the measurement.

Fluorescence Spectroscopy

Fluorescence measurements were carried out at 25 °C using a Hitachi F-4500 or F-7000 spectrophotometer. The emission spectra of tryptophan (Trp, W) were recorded in a 4 × 4 mm cuvette from 300 to 420 nm at the excitation wavelength of 295 nm with increasing concentrations of SUV. To avoid the light scattering caused by SUV, polarizers (excitation and emission polarization set to horizontal and vertical, respectively) were used as described [18]. Contributions from the buffer and SUV without peptide were subtracted from the experimental spectra. The wavelength of maximum fluorescence (WMF) was determined by the first derivation of the spectrum, at which the slope of the curve yields the value close to zero. The free to bound peptide ratio was calculated from the changes in WMF. Assuming that the binding occurs in a saturable manner as indicated in the following equation,

$$P_b/[PC] = B_{max} \cdot P_f/(K_d + P_f)$$

data were analyzed by Hanes-Woolf plot analysis. In this equation, P_f and P_b are the free and bound peptide concentrations, respectively, $[PC]$ is the concentration of PC, B_{max} is the binding maximum, and K_d is the dissociation constant.

DMPC Clearance Assay

Interactions of the apoA-I peptide with DMPC were monitored by the method described [19,20]. DMPC vesicles adjusted to 200 nm in size to prevent sedimentation of vesicles during the measurement, were incubated at 24.6 °C in a thermostated cell holder. The measurements were initiated immediately after the addition of apoA-I peptide or buffer. Sample light scattering intensity was monitored on a SHIMADZU UV-2450 spectrophotometer set at 325 nm.

Table 1.	Primary sequence of apoA-I fragment peptides and their mass	
ApoA-I peptide	Sequence	Found: m/z (Calculated: m + H)
(1–43)	DEPPQSPWDRVKDLATVYVDVLKDSGRDYVSQFEGSALGKQLN	4866.0(4863.4)
(1–43/Y18P)	DEPPQSPWDRVKDLATV**P**VDVLKDSGRDYVSQFEGSALGKQLN	4800.0(4797.4)
(44–65)	LKLLDNWDSVTSTFSKLREQLG	2591.9(2591.4)
(44–65/S55P)	LKLLDNWDSVT**P**TFSKLREQLG	2601.8(2601.4)
(220–241)	PVLESFKVSFLSALEEYTKKLN	2585.8(2583.4)
(220–241/L230P)	PVLESFKVSF**P**SALEEYTKKLN	2568.7(2567.4)
(220–241/F225W)	PVLES**W**KVSFLSALEEYTKKLN	2622.3(2622.4)

Table 2. α-Helix content of apoA-I peptides [a]

ApoA-I peptide	α-Helix (%)		
	Buffer	TFE	SUV
(1−43)	16 ± 1	52 ± 1	42 ± 7
(1−43/Y18P)	17 ± 2	47 ± 3	21 ± 4
(44−65)	12 ± 1	40 ± 2	29 ± 1
(44−65/S55P)	13 ± 1	33 ± 1	18 ± 2
(220−241)	20 ± 2	57 ± 4	49 ± 4
(220−241/L230P)	15 ± 2	44 ± 1	13 ± 1

[a] Mean $\pm$ S.D. from at least three independent experiments.

Isothermal Titration Calorimetry

Enthalpies of apoA-I peptide binding to SUV were measured using a MicroCal MCS isothermal titration calorimeter at 25 °C as described [21]. Measurements were carried out by titrating 5–8 µl aliquots of apoA-I peptide (0.8 mg/ml) into the cell (1.35 ml) containing SUV (15 mM) at constant time intervals of 270 sec. Samples were degassed under vacuum prior to use. Mixing of reactants was accomplished by rotating the syringe paddle at 400 rpm. Enthalpies of binding of apoA-I peptide to SUV were corrected for heat of the peptide dilution and dissociation; these values were determined by titrating the peptide into buffer alone.

Results

CD Measurements

Far-UV CD measurements were performed in solutions and membrane environment. Figure 1 shows typical spectra for apoA-I (1−43) and apoA-I (1−43/Y18P) peptides, and α-helix contents calculated from the molar ellipticity at 222 nm are summarized in Table 2. CD spectra of all the peptides in phosphate buffer showed a single minimum around 200 nm, indicating these peptides being in random coil structure in aqueous solution [22]. In contrast, CD spectra in TFE exhibited double minima at 208 and 222 nm (Figure 1), representing their potential propensity to form α-helix structure. Even apoA-I peptides with a P substitution showed an increase in α-helical content in TFE similarly to the corresponding peptides without a P substitution (Table 2), suggesting that only a single P substitution does not profoundly affect the secondary

structure of the peptides under the condition which compulsorily induces α-helical structure [23].

In the presence of SUV, apoA-I (1−43) and (220−241) peptides showed a significant increase in α-helical content, but they were less than in TFE (Figure 1(a) and Table 2). Compared to these peptides, increase in α-helix content of apoA-I (44−65) peptide upon binding to SUV was relatively small (Table 2), suggesting that apoA-I (44−65) peptide has a lower propensity to form α-helix structure. The addition of SUV caused a negligible effect in α-helix content for apoA-I (1−43/Y18P) and (220−241/L230P) peptides, except for a little increase for apoA-I (44−65/S55P) peptide. α-Helix formation is thought to be a driving force for lipid binding of apolipoproteins [16]. Therefore, this implies that incorporation of the P residue into these peptides impaired the ability to bind to lipid membrane [24].

Trp Fluorescence Measurements

Binding of apoA-I peptides to SUV was also examined by monitoring Trp fluorescence. ApoA-I (1−43) and (44−65) peptides possess an intrinsic Trp residue, W@8 and W@50, respectively. Since apoA-I (220−241) peptide does not have an intrinsic Trp, phenylalanine residue (F@225) was substituted with Trp residue. CD measurements confirmed that there was no significant alteration in the lipid-binding properties by the incorporation of Trp residue at this position. All the peptides in the lipid-free state showed the WMF of 350–355 nm, characteristic of Trp residue in an aqueous environment [25]. This agrees with the CD results showing that these peptides are unstructured in aqueous solution as mentioned above. Addition of SUV into apoA-I (1−43), (44−65), and (220−241/F225W) peptides caused a large increase in fluorescence intensity accompanied by a blue shift in the emission maximum. Such spectral changes are generally explained by the transfer of fluorophore into a less polar and/or motionally more restricted environment [26]. Figure 2(a) shows changes in WMF, an index of environmental changes of Trp residue, as a function of the weight ratio of lipid to peptide. ApoA-I (1−43), (44−65), and (220−241/F225W) peptides exhibited a WMF of around 340 nm at a lipid/peptide ratio of 100 : 1 (w/w), indicating that each Trp residue in these peptides is superficially embedded into a membrane [25]. The dissociation constants, K_d, which reflect the binding affinities, were obtained from Hanes-Woolf plot analysis (Figure 2(b)). ApoA-I (44−65) peptide showed a slightly larger K_d value (11.8 µg/ml) compared to apoA-I (1−43) ($K_d \sim 2.4$ µg/ml) and (220−241/F225W) ($K_d \sim 3.8$ µg/ml) peptides. No significant
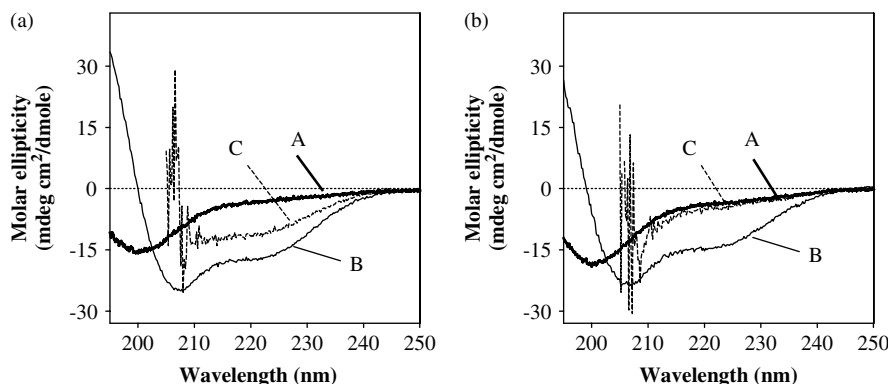

Figure 1. Far-UV CD spectra of (a) apoA-I (1−43) and (b) (1−43/Y18P) peptide in buffer (A), TFE (B), and in the presence of egg PC SUV (C). Peptide concentration was 50 µg/ml. In the mixture of peptide and SUV, lipid to peptide weight ratio was set to 100 : 1.
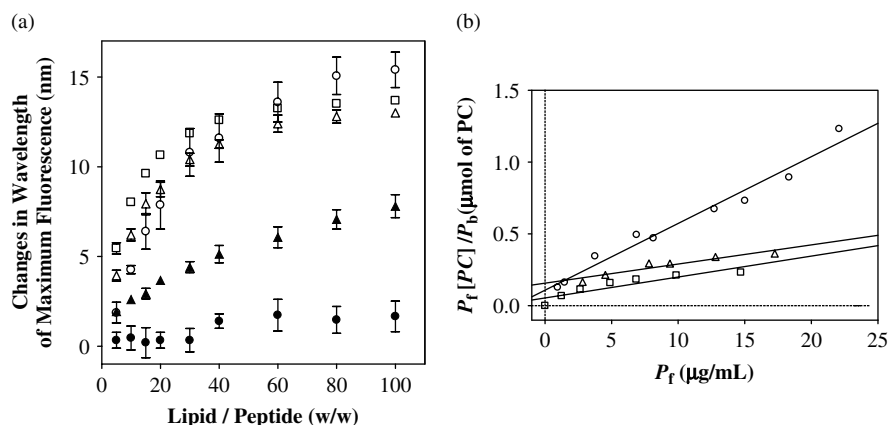
(a)

(b)

Figure 2. (a) Changes in WMF of Trp residue in apoA-I (1–43) (○), (1–43/Y18P) (●), (44–65) (△), (44–65/S55P) (▲), and (220–241/F225W) (□) peptide as a function of PC to peptide weight ratio. Positive value indicates a shift from higher to lower WMF. Peptide concentration was 25 μg/ml. (b) Hanes-Woolf plot analysis of apoA-I (1–43) (○), (44–65) (△), and (220–241/F225W) (□) peptides. $P_f \cdot [PC]/P_b = K_d/B_{max} + P_f/B_{max}$. P_f: free peptide, P_b: bound peptide, $[PC]$: PC concentration, K_d: dissociation constant, B_{max}: binding maximum. K_d is obtained from the X-intercept.

changes were observed in WMF by the addition of SUV into apoA-I (1–43/Y18P) peptide, consistent with CD results (Table 2). This indicates that the most hydrophobic region around Y18 plays a critical role in lipid binding. In contrast, apoA-I (44–65/S55P) peptide showed a moderate shift of WMF, indicative of this peptide still retaining the ability to bind to lipid.

DMPC Clearance Assay

It has been suggested that apoA-I molecule spontaneously generates HDL particles from cell surface lipid domains [27–29]. Similarly, a peptide derived from apoA-I segments is shown to form HDL-like particles [6]. Incubation of apoA-I peptide with phospholipid vesicles at the gel to liquid-crystalline phase transition temperature causes a clarification of the turbidity as a consequence of the formation of HDL-like particles, which is verified by electron microscopy [6,7]. The turbidity of DMPC vesicles was monitored as a function of time. In the absence of apoA-I peptide, there was no change in the turbidity in 300 sec (Figure 3(a)). Addition of apoA-I (1–43) or (220–241) peptide induced a time-dependent decrease in the light-scattering intensity at a concentration of 0.2 mg/ml (Figure 3(a) and (b)),

indicating that these peptides can form discoidal HDL-like particles [30]. ApoA-I (44–65) peptide initially decreased the turbidity, followed by a gradual increase in the turbidity beyond the initial value without a peptide (Figure 3(b)), presumably because of the aggregation of unstable intermediate complexes [31]. The addition of apoA-I (1–43/Y18P) peptide up to 0.4 mg/ml caused no change in turbidity (Figure 3(a)), suggesting that this mutation in the peptide impaired its ability to solubilize lipid vesicles. Collectively, these results indicate that residues around Y18 in apoA-I are required to trigger the binding of the N-terminal domain to lipid [15].

Thermodynamic Measurements

Isothermal titration calorimetry (ITC) was used to measure the binding enthalpy of apoA-I peptide to SUV [32]. The transition from random coil to α-helix structure has been shown to produce a large exothermic heat [16,33,34]. Figure 4 compared the isothermal titration curves of apoA-I peptides injected into SUV, and the obtained binding enthalpies were summarized in Table 3. Titration of apoA-I (1–43) peptide into SUV exhibited a large exothermic heat, whereas little heat was observed for
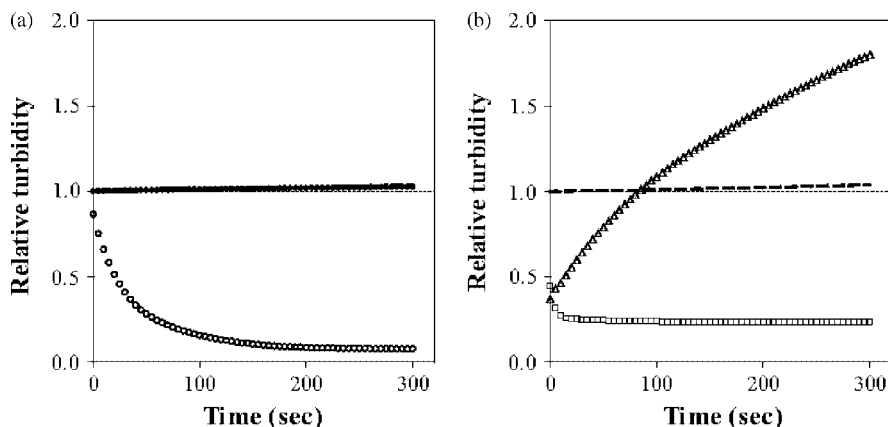
(a)

(b)

Figure 3. Time-dependent clearance of vesicle turbidity monitored by absorbance at 325 nm. DMPC vesicles were incubated at 24.6 °C in the absence (dashed line) and presence of (a) apoA-I (1–43) (○), (1–43/Y18P) (●) and (b) apoA-I (44–65) (△), and (220–241) (□) peptide. PC concentrations were 0.25 mg/ml.

Table 3. Thermodynamic parameters for apoA-I peptide binding to SUV

ApoA-I peptide	ΔH kcal/mol	ΔG kcal/mol	ΔS cal/mol K
(1–43)	−22.4 ± 1.9	−11.0 ± 0.3	−38.3 ± 7.2
(1–43/Y18P)	−1.6 ± 0.3	ND[a]	ND[a]
(44–65)	−7.1 ± 0.2	−9.7 ± 0.2	8.6 ± 1.3
(44–65/S55P)	−3.5 ± 0.1	ND[a]	ND[a]
(220–241)	−6.0 ± 0.7	−10.3 ± 0.4[b]	14.6 ± 3.7
(220–241/L230P)	−0.6 ± 0.1	ND[a]	ND[a]

[a] ND, not determined.
[b] ΔG value was obtained from the dissociation constant of apoA-I (220–241/F225W) peptide.

apoA-I (1–43/Y18P) peptide (Figure 4(a)). This indicates that Y18P mutation in the peptide impairs the formation of α-helical structure upon binding to a lipid membrane, consistent with other spectroscopic measurements. ApoA-I (44–65) and (220–241) peptides exhibited less exothermic heat than that for apoA-I (1–43) peptide (Table 3). Despite the same number of residues and a P substitution in the middle of the sequence, apoA-I (44–65/S55P) peptide yielded a significant amount of binding enthalpy, whereas apoA-I (220–241/L230P) peptide did not.

Discussion

In this study, we examined the role of the N-terminal domain in lipid binding of apoA-I using synthetic peptides. Spectroscopic and thermodynamic measurements revealed that apoA-I (1–43) peptide, but not apoA-I (1–43/Y18P) peptide, has an ability to bind to lipid vesicles, suggesting that the helical segment spanning residues 1–43 is important for lipid binding as well as for maintaining the bundle structure of apoA-I [12]. The present result showing that the Y18P mutation impaired the lipid-binding ability of the peptide seems inconsistent with the previous finding showing that the same mutation enhanced the lipid-binding ability of the protein [15]. This discrepancy could be explained as follows. The most hydrophobic Y18 residue in the N-terminal domain of apoA-I molecule appears to exist in the middle of a helix, contributing to the formation of the N-terminal helix bundle structure. Therefore, the Y18P mutation in the protein induces partial unfolding of the helix bundle. In such a condition, regions

other than the α-helical residues around Y18 would trigger the lipid binding of apoA-I [15].

Compared to apoA-I (1–43) and (220–241) peptides, apoA-I (44–65) peptide exhibited a lower propensity to form α-helical structure, which facilitates lipid binding. In addition, apoA-I (44–65) peptide was able to form HDL-like particles instantaneously but failed to maintain the structure, indicating the length of the helix formed upon lipid binding of this peptide might be too short to stabilize the complexes. In contrast to apoA-I (1–43/Y18P) peptide, apoA-I (44–65/S55P) peptide diminished but not completely impaired the lipid binding, suggesting that either end of this segment can partially form α-helical structure. Although S55 was selected for substitution with proline residue because it is located at the center of residues 44–65, the region around S55 appears not to trigger the α-helix formation to initiate the binding but to be involved in the extension of α-helix structure [35]. Electron paramagnetic resonance spectroscopy of site-directed spin labels indicated that V53 has high degree of motional freedom [36], suggesting that the residues around S55 are unstructured and predicted not to contribute to the helix bundle formation. Taken together, it is feasible that the simplistic punctuation of residues 44–65 based on the sequential analysis [5] is inadequate in terms of the function and tertiary structure of apoA-I.

The entropy of binding (ΔS) was obtained from the enthalpy (ΔH) and the free energy (ΔG) calculated from the binding constant (Table 3). α-Helix formation is an exothermic process, which enthalpically drives the peptide to bind to lipid with high affinity [34]. In fact, the negative ΔH values contributed to the negative ΔG. ApoA-I (44–65) and (220–241) peptides showed positive ΔS values, which arise mainly from enhanced motional freedom of the water molecules. In contrast, apoA-I (1–43) peptide exhibited a negative ΔS value, which is frequently observed in nonclassical hydrophobic interaction [32]. The differences in the energetic contributions to the peptide binding are elusive, but might reflect the differences in the depth of peptide insertion although the Trp fluorescence results showed similar wavelengths upon binding to lipid.

Many naturally occurring mutations of apoA-I associated with abnormal lipid metabolism or amyloidosis have been identified [37]. Mutations in the N-terminal and the central regions are likely to be related to the destabilization of the protein structure and the loss of ability to activate lecithin–cholesterol acyltransferase [9]. In contrast, very few mutations have been described in the C-terminal region that is essential in lipid binding. The present results showing that only a single-point mutation in the sequence,
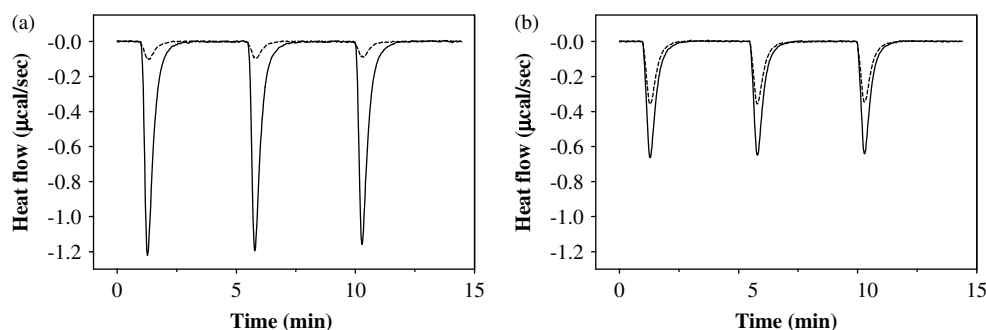

Figure 4. Isothermal titration calorimetry for (a) apoA-I (1–43) (solid line) and (1–43/Y18P) (dotted line) peptide, and (b) apoA-I (44–65) (solid line) and (44–65/S55P) (dotted line) peptide injected into SUV. Lipid particles (15 mM PC) were placed into the sample cell (1.35 ml) and titrated with 5–8 µl aliquots of the apoA-I peptide (0.8 mg/ml) with continual stirring at 400 rpm. The heat generated upon binding of the peptide to SUV was calculated by subtracting the dilution heat.

especially in residues 220–241, led to the complete loss of the lipid-binding ability appears to be relevant to mutations in the putative C-terminal α-helical segment. In fact, apoA-I Nichinan, in which glutamic acid 235 is missing (E235 → 0), has been found to be associated with low HDL levels [38].

Recent X-ray crystallographic analysis revealed that lipid-free apoA-I is folded into two domains; an N-terminal antiparallel helix bundle domain and a discrete C-terminal domain [13]. Upon a binding of the C-terminal domain to lipid membrane, the N-terminal helix bundle is required to be unfolded [39]. Initial lipid binding occurs through the C-terminal domain, which is supposed to induce conformational opening of the helix bundle [12]. Spatial rearrangement of the C-terminal domain upon lipid binding may be recognized by the N-terminal domain, which is considered to interact with the C-terminal domain in the lipid-free state [40,41]. As a result, the N-terminal helix bundle might be partially unfolded, and each of the helices in the bundle including residues 1–43 becomes available for interaction with lipid. The present results together with our previous observations [15] indicate that the most N-terminal region of apoA-I contributes not only to the formation of the N-terminal helix bundle but also to the interaction with lipid through the hydrophobic α-helical residues.

Acknowledgements

References

1. Lewis GF, Rader DJ. New insights into the regulation of HDL metabolism and reverse cholesterol transport. *Circ. Res.* 2005; **96**: 1221–1232.
2. Lewis GF. Determinants of plasma HDL concentrations and reverse cholesterol transport. *Curr. Opin. Cardiol.* 2006; **21**: 345–352.
3. Navab M, Anantharamaiah GM, Reddy ST, Van Lenten BJ, Datta G, Garber D, Fogelman AM. Human apolipoprotein A-I and A-I mimetic peptides: potential for atherosclerosis reversal. *Curr. Opin. Lipidol.* 2004; **15**: 645–649.
4. Navab M, Anantharamaiah GM, Reddy ST, Fogelman AM. Apolipoprotein A-I mimetic peptides and their role in atherosclerosis prevention. *Nat. Clin. Pract. Cardiovasc. Med.* 2006; **3**: 540–547.
5. Segrest JP, Jones MK, De Loof H, Brouillette CG, Venkatachalapathi YV, Anantharamaiah GM. The amphipathic helix in the exchangeable apolipoproteins: a review of secondary structure and function. *J. Lipid Res.* 1992; **33**: 141–166.
6. Palgunachari MN, Mishra VK, Lund-Katz S, Phillips MC, Adeyeye SO, Alluri S, Anantharamaiah GM, Segrest JP. Only the two end helixes of eight tandem amphipathic helical domains of human apo A-I have significant lipid affinity. Implications for HDL assembly. *Arterioscler. Thromb. Vasc. Biol.* 1996; **16**: 328–338.
7. Mishra VK, Palgunachari MN, Datta G, Phillips MC, Lund-Katz S, Adeyeye SO, Segrest JP, Anantharamaiah GM. Studies of synthetic peptides of human apolipoprotein A-I containing tandem amphipathic alpha-helixes. *Biochemistry* 1998; **37**: 10313–10324.
8. Natarajan P, Forte TM, Chu B, Phillips MC, Oram JF, Bielicki JK. Identification of an apolipoprotein A-I structural element that mediates cellular cholesterol efflux and stabilizes ATP binding cassette transporter A1. *J. Biol. Chem.* 2004; **279**: 24044–24052.
9. Frank PG, Marcel YL. Apolipoprotein A-I: structure-function relationships. *J. Lipid Res.* 2000; **41**: 853–872.
10. Saito H, Lund-Katz S, Phillips MC. Contributions of domain structure and lipid interaction to the functionality of exchangeable human apolipoproteins. *Prog. Lipid Res.* 2004; **43**: 350–380.
11. Davidson WS, Hazlett T, Mantulin WW, Jonas A. The role of apolipoprotein AI domains in lipid binding. *Proc. Natl. Acad. Sci. U.S.A.* 1996; **93**: 13605–13610.
12. Saito H, Dhanasekaran P, Nguyen D, Holvoet P, Lund-Katz S, Phillips MC. Domain structure and lipid interaction in human apolipoproteins A-I and E, a general model. *J. Biol. Chem.* 2003; **278**: 23227–23232.
13. Ajees AA, Anantharamaiah GM, Mishra VK, Hussain MM, Murthy HM. Crystal structure of human apolipoprotein A-I: insights into its protective effect against cardiovascular diseases. *Proc. Natl. Acad. Sci. U.S.A.* 2006; **103**: 2126–2131.
14. Chou PY, Fasman GD. Prediction of protein conformation. *Biochemistry* 1974; **13**: 222–245.
15. Tanaka M, Dhanasekaran P, Nguyen D, Ohta S, Lund-Katz S, Phillips MC, Saito H. Contributions of the N- and C-terminal helical segments to the lipid-free structure and lipid interaction of apolipoprotein A-I. *Biochemistry* 2006; **45**: 10351–10358.
16. Saito H, Dhanasekaran P, Nguyen D, Deridder E, Holvoet P, Lund-Katz S, Phillips MC. α-Helix formation is required for high affinity binding of human apolipoprotein A-I to lipids. *J. Biol. Chem.* 2004; **279**: 20974–20981.
17. Egashira M, Gorbenko G, Tanaka M, Saito H, Molotkovsky J, Nakano M, Handa T. Cholesterol modulates interaction between an amphipathic class A peptide, Ac-18A-NH$_2$, and phosphatidylcholine bilayers. *Biochemistry* 2002; **41**: 4165–4172.
18. Ladokhin AS, Jayasinghe S, White SH. How to measure and analyze tryptophan fluorescence in membranes properly, and why bother? *Anal. Biochem.* 2000; **285**: 235–245.
19. Segall ML, Dhanasekaran P, Baldwin F, Anantharamaiah GM, Weisgraber KH, Phillips MC, Lund-Katz S. Influence of apoE domain structure and polymorphism on the kinetics of phospholipid vesicle solubilization. *J. Lipid Res.* 2002; **43**: 1688–1700.
20. Tanaka M, Koyama M, Dhanasekaran P, Nguyen D, Nickel M, Lund-Katz S, Saito H, Phillips MC. Influence of tertiary structure domain properties on the functionality of apolipoprotein A-I. *Biochemistry* 2008; **47**: 2172–2180.
21. Tanaka M, Saito H, Dhanasekaran P, Wehrli S, Handa T, Lund-Katz S, Phillips MC. Effects of the core lipid on the energetics of binding of apoA-I to model lipoprotein particles of different sizes. *Biochemistry* 2005; **44**: 10689–10695.
22. Zhu HL, Atkinson D. Conformation and lipid binding of a C-terminal (198–243) peptide of human apolipoprotein A-I. *Biochemistry* 2007; **46**: 1624–1634.
23. Li SC, Goto NK, Williams KA, Deber CM. Alpha-helical, but not beta-sheet, propensity of proline is determined by peptide environment. *Proc. Natl. Acad. Sci. U.S.A.* 1996; **93**: 6676–6681.
24. Ponsin G, Hester L, Gotto AM Jr, Pownall HJ, Sparrow JT. Lipid-peptide association and activation of lecithin : cholesterol acyltransferase. Effect of alpha-helicity. *J. Biol. Chem.* 1986; **261**: 9202–9205.
25. Clayton AH, Sawyer WH. The structure and orientation of class-A amphipathic peptides on a phospholipid bilayer surface. *Eur. Biophys. J.* 1999; **28**: 133–141.
26. Lakowicz J. *Principles of Fluorescent Spectroscopy*. Kluwer Academic / Plenum Publishers: New York, 1999.
27. Gillotte KL, Zaiou M, Lund-Katz S, Anantharamaiah GM, Holvoet P, Dhoest A, Palgunachari MN, Segrest JP, Weisgraber KH, Rothblat GH, Phillips MC. Apolipoprotein-mediated plasma membrane microsolubilization. Role of lipid affinity and membrane penetration in the efflux of cellular cholesterol and phospholipid. *J. Biol. Chem.* 1999; **274**: 2021–2028.
28. Massey JB, Pownall HJ. Role of oxysterol structure on the microdomain-induced microsolubilization of phospholipid membranes by apolipoprotein A-I. *Biochemistry* 2005; **44**: 14376–14384.
29. Fukuda M, Nakano M, Sriwongsitanont S, Ueno M, Kuroda Y, Handa T. Spontaneous reconstitution of discoidal HDL from sphingomyelin-containing model membranes by apolipoprotein A-I. *J. Lipid Res.* 2007; **48**: 882–889.
30. Zhu HL, Atkinson D. Conformation and lipid binding of the N-terminal (1–44) domain of human apolipoprotein A-I. *Biochemistry* 2004; **43**: 13156–13164.

41

31. Jiang ZG, Gantz D, Bullitt E, McKnight CJ. Defining lipid-interacting domains in the N-terminal region of apolipoprotein B. *Biochemistry* 2006; **45**: 11799–11808.

32. Gazzara JA, Phillips MC, Lund-Katz S, Palgunachari MN, Segrest JP, Anantharamaiah GM, Snow JW. Interaction of class A amphipathic helical peptides with phospholipid unilamellar vesicles. *J. Lipid Res.* 1997; **38**: 2134–2146.

33. Seelig J. Thermodynamics of lipid-peptide interactions. *Biochim. Biophys. Acta* 2004; **1666**: 40–50.

34. Wieprecht T, Apostolov O, Beyermann M, Seelig J. Thermodynamics of the alpha-helix-coil transition of amphipathic peptides in a membrane environment: implications for the peptide-membrane binding equilibrium. *J. Mol. Biol.* 1999; **294**: 785–794.

35. Yang ST, Lee JY, Kim HJ, Eu YJ, Shin SY, Hahm KS, Kim JI. Contribution of a central proline in model amphipathic alpha-helical peptides to self-association, interaction with phospholipids, and antimicrobial mode of action. *FEBS J.* 2006; **273**: 4040–4054.

36. Lagerstedt JO, Budamagunta MS, Oda MN, Voss JC. Electron paramagnetic resonance spectroscopy of site-directed spin labels reveals the structural heterogeneity in the N-terminal domain of apoA-I in solution. *J. Biol. Chem.* 2007; **282**: 9143–9149.

37. Sorci-Thomas MG, Thomas MJ. The effects of altered apolipoprotein A-I structure on plasma HDL concentration. *Trends Cardiovasc. Med.* 2002; **12**: 121–128.

38. Han H, Sasaki J, Matsunaga A, Hakamata H, Huang W, Ageta M, Taguchi T, Koga T, Kugi M, Horiuchi S, Arakawa K. A novel mutant, ApoA-I nichinan (Glu235 → 0), is associated with low HDL cholesterol levels and decreased cholesterol efflux from cells. *Arterioscler. Thromb. Vasc. Biol.* 1999; **19**: 1447–1455.

39. Rogers DP, Roberts LM, Lebowitz J, Datta G, Anantharamaiah GM, Engler JA, Brouillette CG. The lipid-free structure of apolipoprotein A-I: effects of amino-terminal deletions. *Biochemistry* 1998; **37**: 11714–11725.

40. Fang Y, Gursky O, Atkinson D. Structural studies of N- and C-terminally truncated human apolipoprotein A-I. *Biochemistry* 2003; **42**: 6881–6890.

41. Tricerri MA, Behling Agree AK, Sanchez SA, Jonas A. Characterization of apolipoprotein A-I structure using a cysteine-specific fluorescence probe. *Biochemistry* 2000; **39**: 14682–14691.